Size Tunable Gold Nanorods Evenly Distributed in the Channels of Mesoporous Silica

Zhi Li,[†] Christian Kübel,[‡] Vasile I. Pârvulescu,[§] and Ryan Richards[†,*]

[†]Department of Chemistry and Geochemistry, Colorado School of Mines, 1500 Illinois Street, Golden, Colorado 80401, [‡]Fraunhofer Institute for Production Technology and Applied Materials Research (IFAM), Wiener Strasse 12, 28359 Bremen, Germany, and [§]Department of Chemical Technology and Catalysis, University of Bucharest, Soseaua Panduri, Bucharest, Romania

ABSTRACT Uniformly distributed gold nanorods in mesoporous silica were synthesized *in situ* by performing a seed-mediated growth process in the channels of SBA-15 which functions as a hard-template to confine the diameter of gold nanorods. By changing the amount of gold precursor, gold nanorods were prepared with a fixed diameter (6−7 nm) and tunable aspect ratios from 3 to 30. Transmission electron microscope and electron tomography were utilized to visualize the gold nanorods supported on one piece of SBA-15 segment and showed a fairly uniform 3-dimensional distribution of gold nanorods within the SBA-15 channels. The longitudinal plasmon resonances of the gold nanorods/SBA-15 composites analyzed by diffuse reflectance UV−vis spectra were found to be tunable depending on the length of gold nanorods. No significant decrease in surface area and/or pore size of the composite was found after growth, indicating the growth process did not disrupt the open mesoporous structure of SBA-15. The combination of the tunable size of the nanorods and their 3-dimensional distribution within the open supporting matrix makes the gold nanorods/SBA-15 composites interesting candidates to systematically study the influence of the aspect ratio of gold nanorods on their properties and potential applications, *i.e.*, catalyst, optical polarizer, and ultrasensitive medical imaging technique.

KEYWORDS: gold nanorods · SBA-15 · composite · tunable-size · *in situ* · electron tomography · seed-mediated growth

Nanorods with tunable aspect ratio have great potential to show unique optical,[1,2] magnetic, electronic, and chemical properties on the basis of their anisotropic structure. Several synthetic methods exist for preparing metallic nanorods, including electrochemical deposition[3] in hard templates,[4] photochemical synthesis,[5] and seed-mediated growth. Gold nanorods with controllable aspect ratios from 2 to 25 have been prepared by seed-mediated growth procedures (SMG).[6−8] Recent mechanistic and kinetic studies showed that the final structure of the gold nanorods was determined by the crystal structure of the gold seeds[9] and that the nanorod growth rate decelerated throughout the initial growth phase.[10] The seed-mediated growth procedure can also be adapted to grow gold nanorods directly on flat solid surfaces by using seeds immobilized on the surface.[11,12] The seed particles were believed to first grow to a minimum diameter of 17 nm before nanorod formation is initiated on a solid surface.[13] However, the diameter of gold nanorods prepared by SMG slightly increases with the aspect ratio. Recent studies have shown nanorod properties depend on both length and diameter, not just aspect ratio.[14] Therefore, it is highly necessary to develop a procedure to fabricate length tunable gold nanorods with exactly the same diameter.

The channels in mesoporous materials, typically with diameters of 2−30 nm, are a class of promising templates to synthesize nanostructured materials[15−17] by controlling the pore size and structure[18,19] using different templates[20] and synthesis procedures.[21,22] Gold nanowires have been synthesized in the channels of mesoporous SBA-15 by hydrogen flow reduction[23,24] and electroless reduction.[25] Because of the well-defined ordered porous structure of SBA-15, gold nanowires formed in the channels of SBA-15 have a uniform diameter which is normally smaller than that of the nanorods prepared by typical seed-mediated methods, especially for the case of high aspect ratio nanorods. However, the length of those gold nanowires are not well defined because the narrow channels in SBA-15, a few nanometers in diameter and several micrometers in length, are not an efficient mass transfer system,[26] which makes the choice of reducing agent an important factor for the synthesis of gold nanostructures within the matrix. Both the high-temperature hydrogen flow[23] and the hydroxylamine used in electroless reduction[25] are relatively strong reduction agents. A fast reduction of the gold precursor in an inefficient mass transfer system

Ⓦ This paper contains enhanced objects available on the Internet at http://pubs.acs.org/journals/ancac3.

*Address correspondence to rrichard@mines.edu, zli@mines.edu.

Received for review March 6, 2008 and accepted May 25, 2008.

Published online June 24, 2008.
10.1021/nn800137x CCC: $40.75

© 2008 American Chemical Society

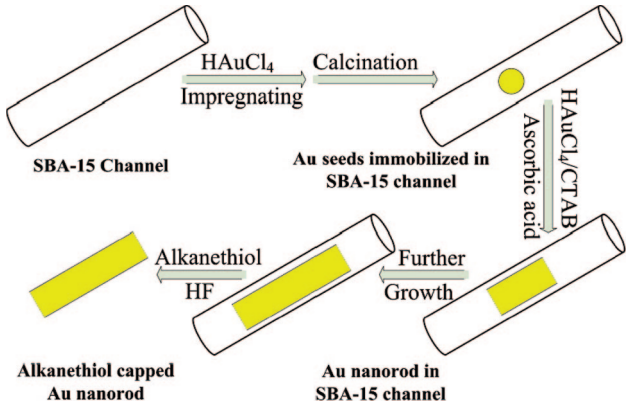

Scheme 1. Synthesis scheme of *in situ* growth of gold nanorods in the channels of SBA-15.

may result in an irregular growth of the nanorods. However it is quite necessary to control the size of gold nanorods to get 3D-gold nanorods in solid matrix. Both theoretical calculation[27] and experimental results[28] showed the 2D periodic arrays of nanorods are high-quality polarizers due to the interactions between nanorods, multipole contributions, and formations of photonic gaps. Therefore it is quite reasonable to expect some interesting applications as optical polarizers from the well-ordered 3D gold nanorods in porous materials as compared with 2D nanorod arrays on a flat solid surface.

In this paper, we have investigated the application of seed-mediated growth to form well-defined nanorods embedded in the channels of SBA-15. By using an appropriate synthetic approach, well defined gold nanorods could be prepared in the SBA-15 channels, and the length of gold nanorods could be tuned by changing the ratio of seed to gold precursor. The formation of gold nanorods and their relatively narrow size distribution were confirmed by both HAADF-STEM (high angle annular dark field scanning transmission electron microscopy) imaging and diffuse reflectance UV−vis spectroscopy. Electron tomography was used to evaluate the 3-D distribution of the gold nanorods in the SBA-15 matrix. The results showed that the nanorods were well distributed within the channels, all roughly parallel to each other throughout the small SBA-15 segment where the curve of pores is normally not significant. This makes the gold nanords/SBA-15 composite an interesting material for optical and catalytic applications. The gold nanorods/SBA-15 composites can be treated as gold heterogeneously immobilized on silica. The catalytic units are well-defined gold nanorods with fixed diameter and tunable length which have a strong contact with the walls of the SBA-15 pores without blocking the open system of SBA-15 due to the existence of micropores perpendicular to the main pores in SBA-15 material. This makes them an ideal model to study the influence of shape and size of gold nanoparticles on their catalytic activity.[29] On the other hand, the gold nanorods/SBA-15 composite can also be treated as gold nanorods "suspended" in silica. Compared to the gold nanorods in liquid suspension, the gold nanorods "suspended" in silica have a much higher concentration and preferential orientation. High concentrations are required to obtain strong signals for optical applications especially in ultrasensitive medical imaging techniques.[30] The parallel orientation of gold nanorods in a SBA-15 segment makes it possible to be used as a 3D polarizer.

TABLE 1. Preparation Details of Different Samples

	seeds/ SBA-15 (g)	0.1 M CTAB (ml)	0.067 M HAuCl4 (ml)	0.01 M AgNO3 (ml)	0.1 M ascorbic acid (ml)
rods100/SBA-15	0.1	100	0.2	0.2	0.14
rods40/SBA-15	0.1	100	0.08	0.08	0.055
rods400/SBA-15	0.1	100	0.8	0.8	0.55

RESULTS AND DISCUSSION

The synthetic approach used to prepare length tunable Au nanorods/SBA-15 composites is shown in Scheme 1. Gold nanoparticles, which are working as seeds for the following steps, were formed in the channels of SBA-15 by a simple impregnation method. Different amounts of gold precursor (Table 1) were used to grow the gold nanorods from same amount of seeds to obtain different lengths. Unsupported gold nanorods can be extracted by removing the silica matrix with 2% HF and 1% dodecanethiol as ligand.

N_2-Adsorbption data (Table 2) showed decreased values in surface area, pore volume, and mean pore size for APTES-SBA-15 as compared to their parent SBA-15 materials as expected owing to the pore-filling effect.[31] However, only slight differences were found between the APTES-SBA-15, seeds/SBA-15, and the three rods/SBA-15 samples because the density of Au is much higher than SiO_2 and the total volume of the nanorods is no more than 1% of the total pore volume (calculated for a sample containing 6 wt % gold), which implied the growth of nanorods did not block the open porous structure of SBA-15.

The Morphology of Gold Nanorods in SBA-15 Channels. To study the morphology of the Au nanorods embedded

TABLE 2. N_2-Adsorbption Data and Length of Nanorods in Different Samples

	S_{BET} (m^2/g)[a]	V_{BJH} (cc/g)[b]	D_{BJH} (nm)[b]	length of rods (nm)[c]
SBA-15	613	0.899	4.89	
APTES-SBA-15	436	0.721	4.88	
seeds/SBA-15	421	0.697	4.93	3−5 (spheres)
rods40/SBA-15	400	0.662	4.88	20−30
rods100/SBA-15	372	0.691	4.83	30−50
rods400/SBA-15	410	0.654	5.53	100−200

[a]The surface area S_{BET} is calculated by BET method. [b]The pore volume and the pore size distribution are determined by the BJH model applied to the desorption branch of isotherm. [c]The length of nanorods is determined by TEM.

in SBA-15, high angle annular dark field scanning TEM (HAADF-STEM) imaging was used, as Z-contrast offers a better gold/silica contrast compared to bright field (BF)-TEM. Figure 1A shows the HAADF-STEM image of Au seeds/SBA-15 prepared by impregnation method. In the Z-contrast images, the Au seeds appear as bright dots with a diameter of 3−5 nm in the pores of the SBA-15. The inset is STEM image of a SBA-15 particle with the orientation of [001] zone axis, which clearly shows the hexagonal pores. The average pore distance is measured to be 9.3 nm which corresponds to the sum of pore diameter and wall thickness.

After performing the seed-mediated growth process, gold nanorods were observed in the channels of SBA-15. Figure 1B shows an overview of the rods100/SBA-15 sample. A large amount of short gold nanorods (the bright rods, which were shown to be gold nanorods by EDX analysis, see Figure S3 in Supporting Information) embedded in a portion of SBA-15 with dimensions of about 1 μm × 3 μm were observed. Those short Au nanorods have a fairly uniform size and are oriented parallel to each other. From the BF-TEM inset of a thin edge of a SBA-15 particle, it can be clearly seen that the gold nanorods are oriented parallel to the channels in the SBA-15. The measured diameter of the gold nanorods is typically in the range of 6−7 nm which is 2−3 nm smaller than the average pore distance of SBA-15(Figure 1A). This suggests that the gold nanorods are dominantly growing inside a single pore of the SBA-15. Nevertheless, depending on the crystallographic orientation of the SBA-15 in the individual (S)TEM image, it might appear as if the gold nanorods are actually bigger than the pores due to the projection of the hexagonal pore structure, for example, close to the [110] or [210] zone axis orientation.

The extraction of gold nanorods from a mesoporous matrix is important for the application of nanorods as building blocks for nanodevices and to allow further characterization. Here, the gold nanorods were extracted by etching the silica matrix with 2% HF. The Au nanorods extracted from rods100/SBA-15 exhibit a uniform diameter around 6−7 nm and an average length of about 30−40 nm. In addition to the Au nanorods, a few large particles can also be seen in Figure 1C. We believed that those particles formed in solution rather than in the channels of SBA-15 and were physically absorbed on the external surface of the SBA-15 template. From the high magnification image (Figure 1D), one can see that the gold nanorods are crystalline and exhibit the characteristic lattice spacings of gold.

We noted that the diameter of the gold nanorods is slightly bigger than the size of SBA-15 pores determined by the BJH model applied to the desorption branch of isotherm. With the STEM images (Figure 1A and Figure 2A), it is hard to judge the exact diameter of pores or the thickness of walls due to the relative poor contrast. But the average pore distance (the sum of pore diameter and wall thickness) can be accurately measured to be around 9.3 nm by the STEM which is significantly bigger than the typical diameter of gold nanorods. In addition, no distortion of SBA-15 ordered pores was observed in the area where the gold nanorods were formed. That suggests the nanorods fit well inside a single channel of the SBA-15 with a remaining pore wall thickness of 2−3 nm.

3D-Reconstruction of Au Nanorods in SBA-15 Channels. Due to the limitations of 2D imaging, it is hard to judge how the nanoscale gold rods are distributed in the layers of the nanoscale channels of the SBA-15 microcrystals by traditional TEM. Electron tomography[32] (3D TEM) was used to visualize a SBA-15 particle around 0.4 μm × 0.4 μm × 0.4 μm including all gold nano-

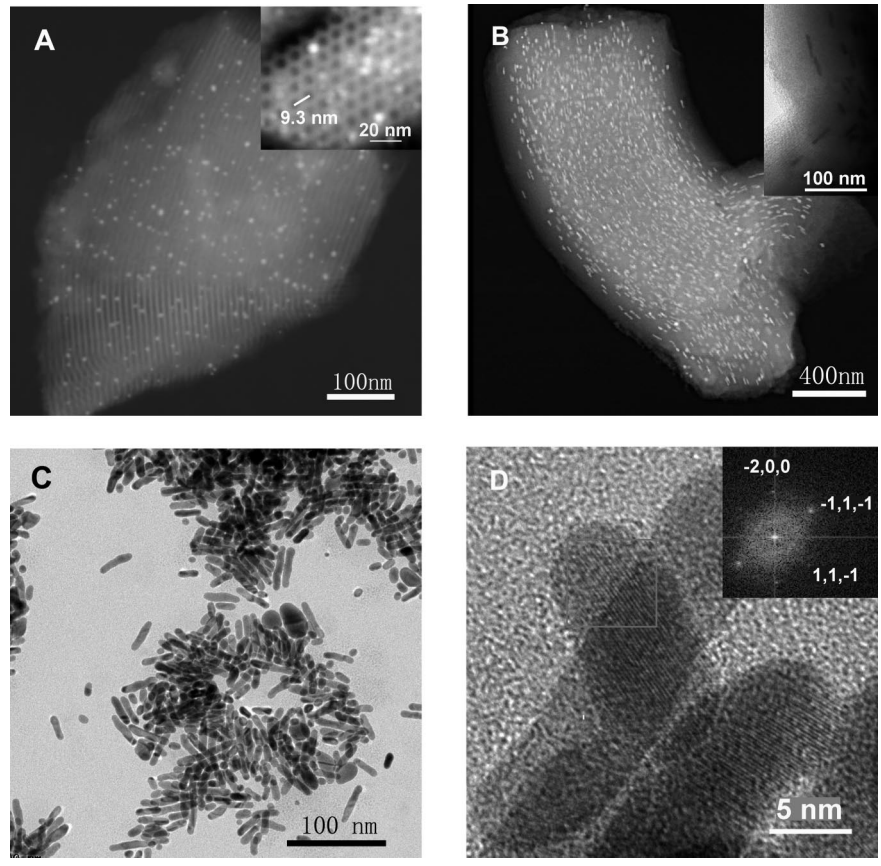

Figure 1. HAADF-STEM images of the (A) seeds/SBA-15 and (B) rods100/SBA-15 (inset is a BF-TEM image at higher magnification); (C) BF-TEM image of unsupported Au rods after removing silica matrix; and (D) HR-TEM image of single-crystalline domain at unsupported Au rods (the inset shows the corresponding fast Fourier transform of the area indicated).

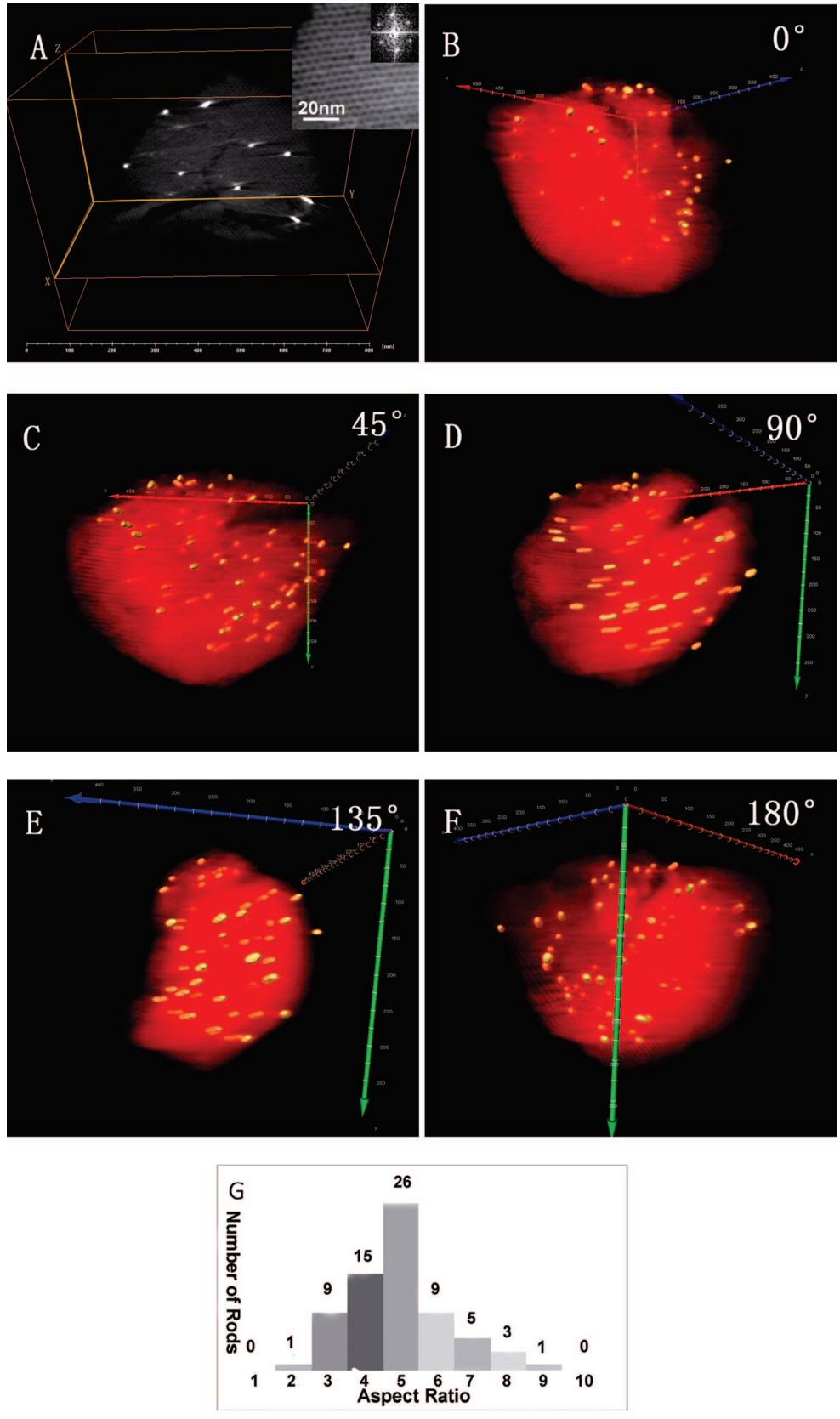

Figure 2. Tomography visualization of rods100/SBA-15: (A) digital slices though the reconstructed volume (the inset is the fast Fourier transform of order porous structure of SBA-15); (B–F) overall visualization of the gold nanorods embedded in a small piece of SBA-15 viewed from diffrent directions; and (G) the aspect ratio statistics of the rods.

Ⓦ A short movie of the 3D visualization of gold nanorods/SBA-15 which shows the overall distribution of gold, video 1, is available.

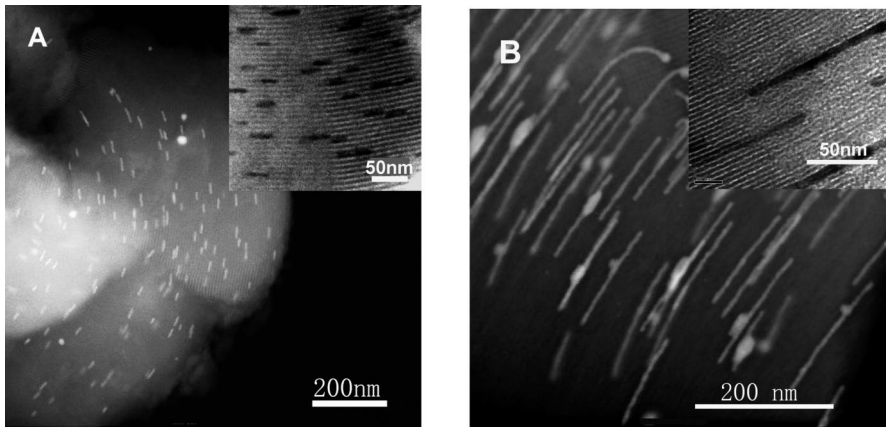

Figure 3. HAADF-STEM images of the (A) rods40/SBA-15 and (B) rods400/SBA-15. The insets are the BF-TEM images at higher magnification.

rods embedded in it (for details see experimental section). The digital slices through the reconstructed volume in Figure 2A show the ordered porous structure of the SBA-15 matrix with several nanorods embedded. The inset image is oriented close to the [001] zone axis in SBA-15 and the corresponding fast Fourier transform (FFT) shows the well-known hexagonal symmetry of SBA-15 with the {110} reflections corresponding to distances of 8.0−8.3 nm. The differences between the observed lattice spacings are related to a slight misorientation of the digital slice with respect to the [001] zone axis, which results in observed real space lattice spacings that are slightly overestimated. Therefore, based on the smallest observed lattice spacing, the average pore distance in SBA-15 is calculated to be 9.2 nm agreeing well with that of seeds/SBA-15 (Figure 1A). That indicates the growth of gold nanorods did not affect the porous structure of SBA-15.

In the overall visualization of Au rods100/SBA-15, the SBA-15 matrix is displayed as volume rendering in red and the gold nanorods are displayed as surface rendering in yellow. When observed from the view parallel to the SBA-15 channels (Figure 2B), only the sphere-like ends of the gold nanorods can be observed. With the rotation of the whole system around the *Y* axis (green) the uniform gold nanorods, 40−50 nm in length (Figure 2D,G), are found to be evenly distributed throughout the entire SBA-15 portion. Several very short nanorods can also been found at the top, which we believe were absorbed on the external surface rather than formed in the channels of SBA-15. This electron tomography clearly shows that the uniform gold nanorods are evenly distributed throughout the SBA-15 support (see video 1).

The Tunable Length of Au Nanorods in SBA-15 Channels. One of the advantages of using the seed-mediated growth method is the tunability of the aspect ratio by varying the ratio of seeds to gold precursor, which makes this method very attractive since the longitudinal plasmon wavelength of elongated nanostructures is strongly dependent on the aspect ratio. However, the diameter of the nanorods also increases with the aspect ratio in a typical seed-mediated growth process.[7,8] Figure 3 shows the growth results in the channels of SBA-15 by using the same amount of seeds but various amounts of gold precursor compared to the sample rods100/SBA-15. The gold nanorods formed using 40% gold precursor (rods40/SBA-15) were around 20−30 nm (Figure 3A), slightly shorter than in rods100/SBA-15 (Figure 2B-D), while long nanorods (rods400/SBA-15), typically around 200 nm, were formed using 400% gold precursor (Figure 3B). However it is hard to judge the length of gold nanorods because of the influence of orientation which can be clearly seen from Figure 2B−F. No variation of the diameter of the gold nanorods was found during the length tuning. From Figure 2C, Figure S2A and Figure S2B, it can be concluded that all nanorods maintained a diameter of 6−7 nm. In Figure 3B, some parts of the nanorods are significantly thicker than other parts, which might be caused by the filling effects. The growth of the long gold nanorods expand the pores of SBA-15, partially breaking the wall where it is less solid and form some gold in adjacent pores. This also explains why the pore size of sample rods400/SBA-15 is larger than its parent SBA-15(Table 2).

The optical properties of the Au/SBA-15 composites were studied by diffuse-reflective UV−vis (Figure 4). Seeds/SBA-15 showed a single surface plasmon resonance peak at 526 nm. The nanorods/SBA-15 composites exhibited the same peaks around 526 nm due to the transverse resonance which are slightly blue-shifted.[6] In addition, longitudinal plasmon resonance peaks were observed at 698 (rods40/SBA-15) and 829 nm (rods400/SBA-15). However, rods400/SBA-15

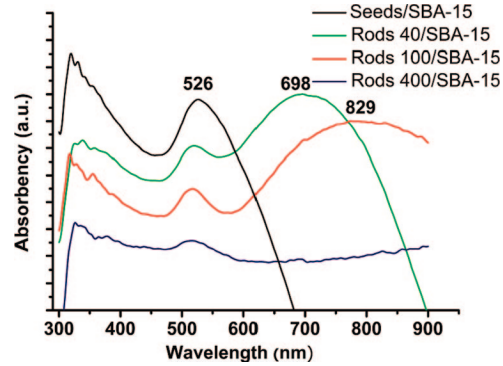

Figure 4. Diffuse-reflectance UV−vis spectra of seeds/SBA-15 and rods/SBA-15 samples with different length.

showed only one peak around 520 nm. Because of their high aspect ratio of more than 20, the longitudinal plasman peak is likely beyond the range of the instrumentation. On the basis of Mie's theory, the plasmon resonances at 628 and 828 nm indicate gold nanorods with aspect ratios of around 3.5 and 5.5. Considering the fixed diameter of those gold nanorods, it can be estimated from the diffuse-reflective UV−vis spectra that the nanorods in rods40/SBA-15 and rods100/SBA-15 have an average length of about 20−25 and 30−40 nm, respectively. The relative sharp longitudinal plasmon resonance peak in the spectrum of rods40/SBA-15 indicates that the gold nanorods prepared using *in situ* growth method have a relative uniform length distribution.

Factors Influencing the Growth Of Au Nanorods. Concentrated CTAB solution has been widely used in the seed-mediated growth of metallic nanorods due to its tendency to form elongated rodlike micellar structures[33] which are believed to play a role as a soft template in the growth process. Though we use a hard template in our work (the pores of SBA-15), the CTAB still played an important role in forming the gold nanorods with high aspect ratio and in controlling their aspect ratio distribution. In experiments performed out using the same procedures to prepare rods 40/SBA-15 and rods 100/SBA-15 but without CTAB, no gold nanorods were formed. The gold nanorods only formed after increasing the amount of gold precursor in the absence of CTAB and the nanorods formed were only about 1/10 to 1/5 of the length compared to the nanorods formed under the same conditions in the presence of CTAB (see Figure S4 in Supporting Materials). One of the possible obstacles to forming uniform gold nanorods in the SBA-15 matrix is the varying mass transfer resistance in the micrometer length channels which leads to different growth rates of gold seeds located at different depths within the channels. However this can be improved if the reducing agent is weak enough so that the reduction process becomes the limiting factor rather than the mass transfer. Ascorbic acid is a weak acid and a recent study shows that the presence of CTAB makes the reduction of the gold precursor a kinetically controlled process.[34] We believe that by the slow reduction of gold in the presence of CTAB, we could eliminate the influence of mass transfer and thus achieve a 3-dimensional uniform growth of the gold seeds embedded in different parts of the SBA-15 channels.

In addition to the importance of the CTAB in solution, the presence of Ag^+ is also critical for the formation of gold nanorods and controlling their aspect ratios.[2,6,7] For preparing rods100/SBA-15 with average aspect ratio 5.5, the initial silver ion concentration is 15% of the concentration of gold. In the final products, the concentration of silver is only 7% of the concentration of gold decided by ICP after digesting Rod100/SBA-15 by HF and aqua regia. This value is closed to the ratio of silver/gold in a typical SMG synthesis.[34] However ICP measurement cannot distinguish between any silver in these samples that might exist as Ag^0, Ag^+, or AgBr on the nanorods surface or SBA-15 surface. In the experiments without the assistance of Ag(I), the resulting gold nanorods showed a poor uniformity (see Figure S5 in Supporting Materials). Besides the gold nanorods, notable amounts of undeveloped gold seeds were observed in the channels and overdeveloped large rods were found at the surface. Ag(I) is known to significantly decrease the growth rate of gold nanorods,[9] and we believe it helped to further reduce the effects of mass transfer limited synthesis. The excess of silver ions in the initial growth solution implies that this reaction is kinetically controlled.

CONCLUSION

This report describes a simple method to prepare uniform gold nanorods in the channels of mesoporous SBA-15. The prepared gold nanorods have a uniform diameter of 6−7 nm and a length tunable to 200 nm. Our interest in this method lays not only in fabricating length tunable ultrafine gold nanorods but also in their potential application, especially as catalysts and optical materials. The gold nanorods/SBA-15 composite, with an open porous structure and length tunable catalyst center (gold nanorods), is a promising model to study the influence of shape on catalytic activity. The high concentration of gold nanorods oriented parallel to each other within each SBA-15 microcrystal could be a good candidate to enhance the signal for optic applications of gold nanorods based on both polarized and nonpolarized light. Further experiments are undergoing.

EXPERIMENTAL SECTION

Materials. Hydrogen tetrachloroaurate ($HAuCl_4 \cdot 3H_2O$, 99.99%), cetyltrimethylammonium bromide (CTAB, 99%), and 3-amimopropyl-triethoxysilane (APTES) were obtained from Sigma. All other reagents were obtained from Aldrich and used as received. Ultrapure deionized water (Continental Water Systems) was used throughout the experiments.

Characterization. Transmission electron microscopy (TEM) was performed at Fraunhofer IFAM, Germany using a FEI Tecnai F20 S-Twin operated in TEM and HAADF-STEM modes at 200 kV with an information limit of 0.15 nm and a nominal spot size of 0.2 nm. Samples were prepared by spreading an ethanol suspension on carbon-coated copper grids and allowing the solvent to evaporate. Electron tomographic data was obtained in HAADF-STEM mode using a single tilt holder to acquire 151 images over a tilt-range of −75° to 75°. IMOD was used to align the tilt-series using a combination of cross-correlation and marker tracking. The 3D reconstruction was performed in Inspect3D using the SIRT algorithm with 25 iterations.

BET and isothermal measurements were performed on a Quantachrome Nova 4000e. Calcination was performed in a tubular furnace with a ramping speed of 3 K per minute. Diffuse re-

flectance UV−vis spectra were recorded on a UV4 (Unicom) spectrophotometer.

Synthesis of APTES-Modified SBA-15 Mesoporous Silica. Mesoporous SBA-15 was prepared as reported in the literature.[35] In a typical synthesis, 4 g of Pluronic123 (triblock copolymer from BASF, EO20.PO70.EO20) was dissolved in 120 mL of 2 M HCl at 40 °C under stirring. After fully dissolving the polymer, 0.041 mol TEOS was added, and stirring was maintained for 24 h at 40 °C. Then the solution was transferred into a Teflon autoclave and kept for 3 days at 95 °C. Afterward, the powder was filtered, dried, and calcined at 550 °C for 8 h, resulting in template-free SBA-15. To modify the surface, 2 g of the prepared SBA-15 powder was suspended under stirring in 100 mL of APTES ethanol solution (1 wt %) for 3 h, and then carefully filtered, washed with ethanol, and dried at 60 °C. The surface modified SBA-15 is marked as APTES-SBA-15 in this report.

Preparation of Au Seeds Immobilized in SBA-15 Channels. The Au seeds immobilized in SBA-15 channels were prepared *via* an impregnation approach. In a typical experiment, 2 g of APTES-SBA-15 powder was suspended in 200 mL of 1 mM $HAuCl_4$ (aq) solution and stirring was maintained for 2 h. Then the solid was filtered out and rinsed three times with deionized water. After calcination at 350 °C for 3 h, a light pink powder (the characteristic color of gold nanoparticles) was obtained (seeds/APTES-SBA-15).

Growth of Gold Nanorods in SBA-15 Channels. Gold nanorods were prepared by a modified seed-mediated growth method. Specifically, 0.1 g of Au seeds/SBA-15 powder was suspended in 100 mL of 0.1 M CTAB (aq) by stirring in an ultrasonic bath for 3 min. The well dispersed seeds/SBA-15 slurry was important for the uniform growth of gold nanorods. A 0.2 mL portion of 0.01 M $AgNO_3$ aqueous solution, 0.2 mL of 0.067 M $HAuCl_4$ trihydrate (aq), and 0.14 mL of 0.1 M ascorbic acid (aq) were added consecutively, with continuous stirring. To ensure full formation of gold nanorods, 24 h reaction time was used, after which the solid powder was filtered from the mixture, rinsed three times with deionized water and ethanol to remove the CTAB and dried at 95 °C. Finally, a red powder was obtained. This powder was marked as rods100/SBA-15 ("100" indicates the relative ratio of gold precursor/seeds). Rods40/SBA-15 and rods400/SBA-15 were prepared in the same way but with different ratios of gold precursor to seed in the growth solution (see Table 1 for details). In the experiment, the Au/ascorbic acid and Au/Ag ratio in the nanorods synthesis solution was kept constant. The numbers (100, 40, 400) in sample names indicate just the relative amount of gold precursor used to prepare the samples and does not mean the actual ratio of gold precursor/gold seeds. With the increase of the gold precursor to seed ratio, the color of the final product varied from pink to gray.

To extract gold nanorods, aqueous HF (46 wt %) was diluted to 2 wt % with ethanol, and to this solution was added 1 wt % of 1-dodecanethiol as ligand. Typically, 5 mg of gold nanorods/SBA-15 composite was dissolved in 10 mL of etching solution. After a few minutes stirring, the solution turned pink or pale (depends on the length of rods), and precipitation was found. The precipitation is redispersible in the solution after 10 min of sonication.

Acknowledgment. The authors gratefully acknowledge Jacobs University Bremen (formerly International University Bremen) for funding, Fraunhofer IFAM, Germany, and Colorado School of Mines.

Supporting Information Available: More characterizations of gold rods/SBA-15 and unsupported gold nanorods including XRD, EDX, and more TEM images. This material is available free of charge *via* the Internet at http://pubs.acs.org.

REFERENCES AND NOTES

1. Orendorff, C. J.; Gole, A.; Sau, T. K.; Murphy, C. J. Surface-Enhanced Raman Spectroscopy of Self-Assembled Monolayers: Sandwich Architecture and Nanoparticle Shape Dependence. *Anal. Chem.* **2005**, *77*, 3261–3266.
2. Nikoobakht, B.; El-Sayed, M. A. Surface-Enhanced Raman Scattering Studies on Aggregated Gold Nanorods. *J. Phys. Chem. A* **2003**, *107*, 3372–3378.
3. Yu, Y. Y.; Chang, S. S.; Lee, C. L.; Wang, C. R. C. Gold Nanorods: Electrochemical Synthesis and Optical Properties. *J. Phys. Chem. B* **1997**, *101*, 6661–6664.
4. van der Zande, B. M. I.; Bohmer, M. R.; Fokkink, L. G. J.; Schonenberger, C. Colloidal Dispersions of Gold Rods: Synthesis and Optical Properties. *Langmuir* **2000**, *16*, 451–458.
5. Esumi, K.; Matsuhisa, K.; Torigoe, K. Preparation of Rodlike Gold Particles by UV Irradiation Using Cationic Micelles as a Template. *Langmuir* **1995**, *11*, 3285–3287.
6. Jana, N. R.; Gearheart, L.; Murphy, C. J. Seed-Mediated Growth Approach for Shape-Controlled Synthesis of Spheroidal and Rod-Like Gold Nanoparticles Using a Surfactant Template. *Adv. Mater.* **2001**, *13*, 1389–1393.
7. Jana, N. R.; Gearheart, L.; Murphy, C. J. Wet Chemical Synthesis of High Aspect Ratio Cylindrical Gold Nanorods. *J. Phys. Chem. B* **2001**, *105*, 4065–4067.
8. Busbee, B. D.; Obare, S. O.; Murphy, C. J. An Improved Synthesis of High-Aspect-Ratio Gold Nanorods. *Adv. Mater.* **2003**, *15*, 414–416.
9. Liu, M. Z.; Guyot-Sionnest, P. Mechanism of Silver(I)-Assisted Growth of Gold Nanorods and Bipyramids. *J. Phys. Chem. B* **2005**, *109*, 22192–22200.
10. Gulati, A.; Liao, H.; Hafner, J. H. Monitoring Gold Nanorod Synthesis by Localized Surface Plasmon Resonance. *J. Phys. Chem. B* **2006**, *110*, 22323–22327.
11. Taub, N.; Krichevski, O.; Markovich, G. Growth of Gold Nanorods on Surfaces. *J. Phys. Chem. B* **2003**, *107*, 11579–11582.
12. Mieszawska, A. J.; Slawinski, G. W.; Zamborini, F. P. Directing the Growth of Highly Aligned Gold Nanorods Through a Surface Chemical Amidation Reaction. *J. Am. Chem. Soc.* **2006**, *128*, 5622–5623.
13. Liao, H. W.; Hafner, J. H. Monitoring Gold Nanorod Synthesis on Surfaces. *J. Phys. Chem. B* **2004**, *108*, 19276–19280.
14. Odom, T. W.; Nehi, C. L. How Gold Nanoparticles Have Stayed in the Light: The 3M's Principle. *ACS Nano* **2008**, *2*, 612–616.
15. Asefa, T.; Lennox, R. B. Synthesis of Gold Nanoparticles via Electroless Deposition in SBA-15. *Chem. Mater.* **2005**, *17*, 2481–2483.
16. Lu, A. H.; Schmidt, W.; Tatar, S. D.; Spliethoff, B.; Popp, J.; Kiefer, W.; Schuth, F. Formation of Amorphous Carbon Nanotubes on Ordered Mesoporous Silica Support. *Carbon* **2005**, *43*, 1811–1814.
17. Wang, Y. Q.; Yang, C. M.; Schmidt, W.; Spliethoff, B.; Bill, E.; Schuth, F. Weakly Ferromagnetic Ordered Mesoporous Co_3O_4 Synthesized by Nanocasting From Vinyl-Functionalized Cubic Ia3d Mesoporous Silica. *Adv. Mater.* **2005**, *17*, 53–55.
18. Lu, A. H.; Li, W. C.; Kiefer, A.; Schmidt, W.; Bill, E.; Fink, G.; Schuth, F. Fabrication of Magnetically Separable Mesostructured Silica with an Open Pore System. *J. Am. Chem. Soc.* **2004**, *126*, 8616–8617.
19. Yang, C. M.; Schmidt, W.; Kleitz, F. Pore Topology Control of Three-Dimensional Large Pore Cubic Silica Mesophases. *J. Mater. Chem.* **2005**, *15*, 5112–5114.
20. Hawkins, K. M.; Wang, S. S. S.; Ford, D. M.; Shantz, D. F. Poly-L-Lysine Templated Silicas: Using Polypeptide Secondary Structure to Control Oxide Pore Architectures. *J. Am. Chem. Soc.* **2004**, *126*, 9112–9119.
21. Kim, T. W.; Kleitz, F.; Paul, B.; Ryoo, R. MCM-48-Like Large Mesoporous Silicas with Tailored Pore Structure: Facile Synthesis Domain in a Ternary Triblock Copolymer-Butanol-Water System. *J. Am. Chem. Soc.* **2005**, *127*, 7601–7610.
22. Kleitz, F.; Solvyov, L. A.; Anilkumar, G. M.; Choi, S. H.; Ryoo, R. Transformation of Highly Ordered Large Pore Silica Mesophases (*Fm3m*, *Im3m* and *P6mm*) In a Ternary Triblock Copolymer-Butanol-Water System. *Chem. Commun.* **2004**, 1536–1537.
23. Gu, J. L.; Shi, J. L.; Xiong, L. M.; Chen, H. R.; Li, L.; Ruan, M. L. A New Strategy to Incorporate High Density Gold Nanowires into the Channels of Mesoporous Silica Thin

Films by Electroless Deposition. *Solid State Sci.* **2004**, *6*, 747–752.
24. Fukuoka, A.; Higuchi, T.; Ohtake, T.; Oshio, T.; Kimura, J.; Sakamoto, Y.; Shimomura, N.; Inagaki, S.; Ichikawa, M. Nanonecklaces of Platinum and Gold with High Aspect Ratios Synthesized in Mesoporous Organosilica Templates by Wet Hydrogen Reduction. *Chem. Mater.* **2006**, *18*, 337–343.
25. Petkov, N.; Stock, N.; Bein, T. Gold Electroless Reduction in Nanosized Channels of Thiol-Modified SBA-15 Material. *J. Phys. Chem. B* **2005**, *109*, 10737–10743.
26. Tian, R. J.; Sun, J. M.; Zhang, H.; Ye, M. L.; Xie, C. H.; Dong, J.; Hu, J. W.; Ma, D.; Bao, X. H.; Zou, H. F. Large-Pore Mesoporous SBA-15 Silica Particles with Submicrometer Size as Stationary Phases for High-Speed CEC Separation. *Electrophoresis* **2006**, *27*, 742–748.
27. Rahachou, A. I.; Zozoulenko, I. V. Light Propagation in Nanorod Arrays. *J. Opt. A-Pure Appl. Opt.* **2007**, *9*, 265–270.
28. McMahon, M. D.; Ferrara, D.; Bowie, C. T.; Lopez, R.; Haglund, R. F. Second Harmonic Generation from Resonantly Excited Arrays of Gold Nanoparticles. *Appl. Phys. B-Lasers Opt.* **2007**, *87*, 259–265.
29. Sau, T. K.; Pal, A.; Pal, T. Size Regime Dependent Catalysis by Gold Nanoparticles for the Reduction of Eosin. *J. Phys. Chem. B* **2001**, *105*, 9266–9272.
30. Wang, H. F.; Huff, T. B.; Zweifel, D. A.; He, W.; Low, P. S.; Wei, A.; Cheng, J. X. *In Vitro* and *in Vivo* Two-Photon Luminescence Imaging of Single Gold Nanorods. *Proc. Natl. Acad. Sci. U.S.A.* **2005**, *102*, 15752–15756.
31. Guari, Y.; Thieuleux, C.; Mehdi, A.; Reye, C.; Corriu, R. J. P.; Gomez-Gallardo, S.; Philippot, K.; Chaudret, B. *In Situ* Formation of Gold Nanoparticles within Thiol Functionalized HMS-C-16 and SBA-15 Type Materials *via* an Organometallic Two-Step Approach. *Chem. Mater.* **2003**, *15*, 2017–2024.
32. Kübel, C.; Voigt, A.; Schoenmakers, R.; Otten, M.; Su, D.; Lee, T. C.; Carlsson, A.; Bradley, J. Recent Advances in Electron Tomography: TEM and HAADF-STEM Tomography for Materials Science and Semiconductor Applications. *Microsc. Microanal.* **2005**, *11*, 378–400.
33. Tornblom, M.; Henriksson, U. Effect of Solubilization of Aliphatic Hydrocarbons on Size And Shape of Rodlike C(16)Tabr Micelles Studied by H-2 NMR Relaxation. *J. Phys. Chem. B* **1997**, *101*, 6028–6035.
34. Orendorff, C. J.; Murphy, C. J. Quantitation of Metal Content in the Silver-Assisted Growth of Gold Nanorods. *J. Phys. Chem. B* **2006**, *110*, 3990–3994.
35. Zhao, D. Y.; Feng, J. L.; Huo, Q. S.; Melosh, N.; Fredrickson, G. H.; Chmelka, B. F.; Stucky, G. D. Triblock Copolymer Syntheses of Mesoporous Silica with Periodic 50 to 300 Angstrom Pores. *Science* **1998**, *279*, 548–552.